High-Rate Space-Time Layered OFDM

Yan Xin and Georgios B. Giannakis [1]
Department of Electrical and Computer Engr.
University of Minnesota
200 Union Street SE
Minneapolis, MN 55455
e-mail: {yxin,georgios}@ece.umn.edu

Abstract — **We derive a layered space-time scheme for multi-antenna orthogonal frequency-division multiplexed transmissions over frequency-selective channels. Compared with existing alternatives, the proposed scheme can attain very high spectral efficiency as well as improved performance. Enhanced multipath diversity gains document its superior performance that is also tested by simulation.**

I. Introduction

Deployment of multiple transmit- and receive-antennas has triggered excitement in basic and applied research, because multi-antenna communications offer the potential to improve performance and capacity of flat- [5], as well as frequency-selective fading channels [2]. When combined with orthogonal frequency division multiplexing (OFDM), multi-antenna transmissions over intersymbol interference (ISI) channels can also afford low-complexity equalization and decoding. Specific multi-antenna systems with OFDM include the Vertical Bell-labs Layered Space-Time (VBLAST) OFDM [8], and the Space-Time Coded (STC) OFDM with ST trellis or block codes [1, 7, 3]. VBLAST-OFDM is "rate-oriented" as it offers high spectral efficiency at an affordable receiver complexity, while STC-OFDM is "performance-oriented" since it is designed to maximize diversity and coding gains. However, the "jack of both trades" is not available: STC-OFDM incurs rate loss that increases with the number of transmit-antennas, while VBLAST-OFDM comes with performance loss because it neither capitalizes fully on transmit-diversity nor it exploits the multipath-diversity that becomes available with ISI channels.

It is the objective of this letter to bridge this gap, and develop a high-rate layered OFDM scheme with high-performance, and flexibility to enable desirable tradeoffs among rate, performance, and receiver complexity. We reach these goals for *frequency-selective* channels by wedding the OFDM subcarrier grouping ideas we put forth in [7], with Linear Constellation Precoding (LCP) tools [4, 10], and the Diagonal (D)BLAST architecture that was originally proposed for *flat-fading* channels in [6]. We describe the system model in Section II; we develop the novel scheme, that we naturally term DBLAST-OFDM-LCP, in Section II; we derive decoders and analyze their performance in Section III.

Notation: Bold lower (upper) case letters are used to denote column vectors (matrices); $(\cdot)^T$ and $(\cdot)^{\mathcal{H}}$ represent transpose and conjugate transpose of a matrix, respectively; $[\cdot]_{ij}$ denotes the (i,j)th entry of a matrix; and $\text{diag}[d_1,\ldots,d_P]$ denotes a diagonal matrix with diagonal entries $d_1,\ldots,d_P$.

II. Precoding, DBLAST, and OFDM

Consider a multi-antenna system with N_t transmit- and N_r receive-antennas, where OFDM transmissions with N_c carriers are employed as depicted in Fig. 1. The fading channel between the mth transmit- and the nth receive-antenna is frequency-selective with discrete-time baseband equivalent finite impulse response (FIR) coefficients collected in the $(L+1)\times 1$ vector $\mathbf{h}_{nm} := [h_{mn}(0),\ldots,h_{mn}(L)]^T$, with $m \in [1,N_t]$, and $n \in [1,N_r]$. We assume that $h_{nm}(l)$'s are independent and identically distributed (i.i.d.), zero-mean, complex Gaussian with variance $1/(2L+2)$ per dimension.

The information symbol stream $\{s_i\}$ is first de-multiplexed to N_t sub-streams, $\{s_{i,m}\}_{m=1}^{N_t}$, one for each transmit-antenna. Every sub-stream, say the mth, is parsed into blocks, each containing N_c symbols, as many as the system carriers. We select $N_c = N_g(L+1)$, and split every block of N_c symbols into N_g groups, each containing $L+1$ symbols. Let $\bar{\mathbf{s}}_m^{(p)}$ denote the pth $N_c\times 1$ such block of the mth sub-stream. The gth group from this block is denoted by $\mathbf{s}_{g,m}^{(p)}$, and is particularly chosen to contain the $L+1$ symbols $\{s_{lN_g+g,m}^{(p)}\}_{l=0}^{L}$. Forming likewise all N_g groups will turn out to reduce decoding complexity, but as we will see later, when this particular grouping is combined with precoding, it will also enable the maximum diversity gains (see also [7]).

Collecting $\mathbf{s}_{g,m}^{(p)}$ blocks across all N_t antennas, we form the $N_t(L+1)\times 1$ vector $\mathbf{s}_g^{(p)} := [\mathbf{s}_{g,1}^{(p)T},\ldots,\mathbf{s}_{g,N_t}^{(p)T}]^T$ on which we apply linear constellation precoding (LCP) to obtain $\mathbf{\Theta}\mathbf{s}_g^{(p)}$, where $\mathbf{\Theta}$ is the $N_t(L+1)\times N_t(L+1)$ LCP matrix. With reference to Fig. 1, and $\boldsymbol{\theta}_{lN_t+m}^T$ denoting the (lN_t+m)th row of $\mathbf{\Theta}$, the (lN_t+m)th entry, $\boldsymbol{\theta}_{lN_t+m}^T\mathbf{s}_g^{(p)}$, of the pth precoded block will form the symbol $l\in[0,L]$ in the gth group of the mth LCP mapper output. Repeating this for all N_g groups of

[1]This work was supported by the NSF Wireless Initiative grant no. 99-79443, and by the ARL/CTA grant no. DAAD19-01-2-011.

$L+1$ symbols, describes how the N_t input blocks indexed by p (containing N_c symbols each) are mapped via LCP to yield N_t output blocks that are also indexed by p, and each contains N_c symbols. Notice that each output symbol is formed as a linear combination of $N_t(L+1)$ symbols from *all* N_t input sub-streams. This is precisely what enables $\mathbf{\Theta}$ to collect both transmit- as well as multipath-diversity gains. If instead of $L+1$ symbols, only one symbol is taken per sub-stream as input to the LCP mapper, then $\mathbf{s}_{g,m}^{(p)}$ reduces to a scalar (call it $s_{n_c,m}^{(p)}$ with $n_c \in [1, N_c]$), the LCP matrix (call it $\bar{\mathbf{\Theta}}$) becomes $N_t \times N_t$, and each LCP output symbol is now a linear combination of N_t input symbols. Because $\bar{\mathbf{\Theta}}$ is smaller than $\mathbf{\Theta}$, this leads to reduced complexity de-precoding, but ensures only full transmit-diversity gain. Consider now a collection of N_l input blocks $\{\bar{\mathbf{s}}_m^{(p)}\}_{p=1}^{N_l}$ per sub-stream, and the corresponding LCP output blocks, each organized in N_g groups as before: $\{\mathbf{\Theta}\mathbf{s}_g^{(p)},\ g \in [1, N_g]\}_{p=1}^{N_l}$. With the latter as N_t-branch input, the DBLAST mapper depicted in Fig. 1 outputs a set of $N_t \times N$ matrices $\{\mathbf{C}_g(l),\ g \in [1, N_g],\ l \in [0, L]\}$, defined as:

$$\mathbf{C}_g(l) := \begin{bmatrix} c_{g,1}^{(1)}(l) & \cdots & c_{g,1}^{(N_l)}(l) & 0 & \cdots & 0 \\ 0 & c_{g,2}^{(2)}(l) & \cdots & c_{g,2}^{(N_l)}(l) & \ddots & 0 \\ \vdots & \ddots & \ddots & \cdots & \ddots & 0 \\ 0 & \cdots & 0 & c_{g,N_t}^{(1)}(l) & \cdots & c_{g,N_t}^{(N_l)}(l) \end{bmatrix}, \quad (1)$$

where the number of columns $N = N_l + N_t - 1$, and $[\mathbf{C}_g(l)]_{mq} := c_{g,m}^{(p)}(l) := \boldsymbol{\theta}_{lN_t+m}^T \mathbf{s}_g^{(p)}$, with $p = q - m + 1$, $q \in [m, N_l + m - 1]$, and "0" otherwise. Notice that $\mathbf{C}_g(l)$ is structurally reminiscent of the DBLAST code matrix with N_l layers (diagonals) [5, 6]. Since $l \in [0, L]$ and $g \in [1, N_g]$, we can use $k = lN_g + g$ to index the N_c LCP-mapper output symbols per block, and re-label each entry $[\mathbf{C}_g(l)]_{mq}$ as $[\mathbf{C}(k)]_{mq}$.

We then feed $\mathbf{c}_{mq} := [[\mathbf{C}(1)]_{mq}, \ldots, [\mathbf{C}(N_c)]_{mq}]^T$ as input to the inverse fast Fourier transform (IFFT) processor of the mth antenna during the qth block (OFDM block-symbol). Next, we take the N_c-point IFFT to obtain $\tilde{\mathbf{c}}_{mq} = \text{IFFT}[\mathbf{c}_{mq}]$, where $[\tilde{\mathbf{c}}_{mq}]_k$ denotes the kth entry of $\tilde{\mathbf{c}}_{mq}$. Prepending the cyclic prefix (CP) of length L, we obtain for each (m, q) an $(N_c + L) \times 1$ block $\bar{\mathbf{c}}_{m,q}$ with entries $\{[\tilde{\mathbf{c}}_{mq}]_{N_c-L+1} \cdots [\tilde{\mathbf{c}}_{mq}]_{N_c} [\tilde{\mathbf{c}}_{mq}]_1 \cdots [\tilde{\mathbf{c}}_{mq}]_{N_c}\}$, that we subsequently digital-to-analog convert, pulse shape, and transmit from the mth antenna during the qth block. Our transmitted $N_t \times N(N_c + L)$ space-time code matrix is:

$$\bar{\mathbf{C}} := \begin{bmatrix} \bar{\mathbf{c}}_{1,1}^T & \bar{\mathbf{c}}_{1,2}^T & \cdots & \bar{\mathbf{c}}_{1,N_l}^T & \mathbf{0}^T & \cdots & \mathbf{0}^T \\ \mathbf{0}^T & \bar{\mathbf{c}}_{2,1}^T & \bar{\mathbf{c}}_{2,2}^T & \cdots & \bar{\mathbf{c}}_{2,N_l}^T & \ddots & \vdots \\ \vdots & \ddots & \ddots & \ddots & \cdots & \ddots & \mathbf{0}^T \\ \mathbf{0}^T & \cdots & \mathbf{0}^T & \bar{\mathbf{c}}_{N_t,1}^T & \bar{\mathbf{c}}_{N_t,2}^T & \cdots & \bar{\mathbf{c}}_{N_t,N_l}^T \end{bmatrix}. \quad (2)$$

All the FIR channels are supposed to remain invariant over $N(N_c + L)$ symbol periods. The number of nonzero block entries $\bar{\mathbf{c}}_{mq}^T$ in $\bar{\mathbf{C}}$ is $N_l N_t = (N - N_t + 1)N_t$; and each $1 \times (N_c + L)$ block entry $\bar{\mathbf{c}}_{mq}^T$ carries N_c information symbols (since L redundant symbols correspond to the CP). With these symbols drawn from the alphabet of size $|\mathcal{A}_s|$, our transmission rate is found to be:

$$R = \frac{N_t(N - N_t + 1)N_c}{N(N_c + L)} \log_2 |\mathcal{A}_s| \quad \text{bps/Hz}. \quad (3)$$

Clearly, selecting $N \gg N_t$ and $N_c \gg L$ leads to very high rates relative to the STC-OFDM schemes in [1, 7, 3]. To appreciate the flexibility and improved performance of our scheme over the high-rate VBLAST-OFDM in [8], we turn to the receiver and consider the input-output relationship per carrier.

We suppose that carrier synchronization, channel acquisition, timing, and symbol-rate sampling have been accomplished successfully at the receiver. We then remove the CP to eliminate the inter-block interference, and subsequently take the N_c-point FFT of each block at the output of each antenna's receive-filter. Recall that the CP insertion and removal along with the IFFT and FFT taken at the transmitters and receivers, respectively, convert the $N_t N_r$ frequency selective channels to a set of $N_t N_r N_c$ flat fading sub-channels. Specifically, the samples of the qth block at the nth receive-filter output obey the following input-output relationship on the kth carrier:

$$y_{nq}(k) = \sum_{m=1}^{N_t} H_{nm}(k)[\mathbf{C}(k)]_{mq} + w_{nq}(k), \quad (4)$$

where $H_{nm}(k)$ is the frequency response of $\mathbf{h}_{nm}$ at the kth carrier, i.e., $H_{nm}(k) = \sum_{l=0}^{L} h_{nm}(l) e^{-j2\pi lk/N_c}$, and $w_{nq}(k)$'s are independent complex Gaussian random variables with zero mean and variance N_0.

Collecting samples $y_{nq}(k)$ from all N_r receive-antennas, and across all N blocks (OFDM block-symbols), for a fixed carrier k, we can recast (4) in a compact matrix form: $\mathbf{Y}(k) = \mathbf{H}(k)\mathbf{C}(k) + \mathbf{W}(k)$, where $[\mathbf{Y}(k)]_{nq} = y_{nq}(k), [\mathbf{H}(k)]_{nm} := H_{nm}(k)$, and $[\mathbf{W}(k)]_{nq} := w_{nq}(k)$. Re-writing k as $k = lN_g + g$, we will pursue decoding per group g, in which the following relationship holds:

$$\mathbf{Y}_g(l) = \mathbf{H}_g(l)\mathbf{C}_g(l) + \mathbf{W}_g(l), \quad (5)$$

where $\mathbf{Y}_g(l) := \mathbf{Y}(lN_g + g)$, $\mathbf{H}_g(l) := \mathbf{H}(lN_g + g)$, $\mathbf{C}_g(l) := \mathbf{C}(lN_g + g)$, and $\mathbf{W}_g(l) := \mathbf{W}(lN_g + g)$.

In a nutshell, we have developed a layered space time system, which can be viewed as a block version of DBLAST that is combined with OFDM to enable high-rate multi-antenna transmissions over frequency selective channels. As the term DBLAST-OFDM-LCP indicates, our scheme relies also on linear constellation precoding. As we will see next, LCP applied to groups of carriers enriches our high-rate OFDM with multipath diversity at an affordable receiver complexity.

III. Decoding and Performance

Suppose that the channels have been acquired at the receiver, and recall from (1) that $[\mathbf{C}_g(l)]_{mq} := \boldsymbol{\theta}_{lN_t+m}^T \mathbf{s}_g^{(q-m+1)}$. We can see that the information symbols in $\mathbf{s}_g := [\mathbf{s}_g^{(1)T} \cdots \mathbf{s}_g^{(N_l)T}]^T$ are spread across all the carriers of group

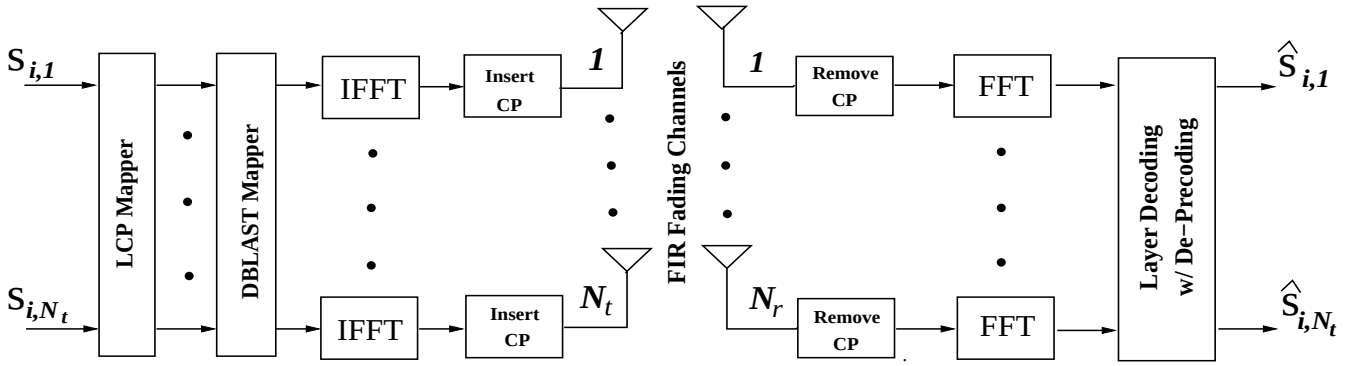

Figure 1: System Model

g. Thus, we need to consider $\mathbf{C}_g := [\mathbf{C}_g(0)\cdots\mathbf{C}_g(L)]$ when decoding $\mathbf{s}_g$. Maximum-likelihood (ML) decoding can then be performed per group of carriers to yield: $\hat{\mathbf{s}}_g = \arg\min_{\mathbf{s}_g}\sum_{l=0}^{L}\|\mathbf{Y}_g(l)-\mathbf{H}_g(l)\mathbf{C}_g(l)\|^2$. Albeit computationally heavy, we prove next that when $\mathbf{\Theta}$ is properly designed, this ML decoding enables the maximum possible diversity order.

Proposition 1 *If the channel taps are i.i.d., and $\mathbf{\Theta}$ is selected so that $\prod_{i=1}^{N_t(L+1)}\boldsymbol{\theta}_i^T\mathbf{e}_g^{(p)}\neq 0$, $\forall\ \mathbf{e}_g^{(p)}:=\mathbf{s}_g^{(p)}-\tilde{\mathbf{s}}_g^{(p)}\neq\mathbf{0}$ with $p=1,\ldots,N_l$, then the maximum diversity order $N_tN_r(L+1)$ can be achieved by ML decoding per group.*

Proof: If $\tilde{\mathbf{C}}_g := [\tilde{\mathbf{C}}_g(0)\cdots\tilde{\mathbf{C}}_g(L)]\neq\mathbf{C}_g$ is decoded instead of $\mathbf{C}_g$, there must exist at least one p such that $\mathbf{e}_g^{(p)}:=\mathbf{s}_g^{(p)}-\tilde{\mathbf{s}}_g^{(p)}\neq\mathbf{0}$. Let p_0 denote the smallest p such that $\mathbf{e}^{(p_0)}\neq\mathbf{0}$. As $\mathbf{\Theta}$ satisfies $\prod_{i=1}^{N_t(L+1)}\boldsymbol{\theta}_i^T\mathbf{e}_g^{(p_0)}\neq 0$ whenever $\mathbf{e}_g^{(p_0)}\neq\mathbf{0}$, it follows from the definition of the entries in (1) that an upper-triangular $N_t\times N_t$ sub-matrix with non-zero diagonal entries in $\mathbf{C}_g(l)-\tilde{\mathbf{C}}_g(l)$ must exist for each l. Thus, $\text{rank}[\mathbf{C}_g(l)-\tilde{\mathbf{C}}_g(l)]=N_t$ for $l\in[0,L]$. Based on the *sum-of-ranks criterion* [7, eq. (25)], we deduce that the achievable diversity order is $G_d:=N_r\sum_{l=0}^{L}\text{rank}[\mathbf{C}_g(l)-\tilde{\mathbf{C}}_g(l)]=N_rN_t(L+1)$. □

Proposition 1 specifies the maximum diversity order that is achieved when the $L+1$ channel taps are i.i.d.; otherwise, $L+1$ in Proposition 1 must be replaced by the minimum rank of the channel correlation matrices $\mathbf{R}_{h,nm}:=E[\mathbf{h}_{nm}\mathbf{h}_{nm}^{\mathcal{H}}]$ for $n\in[1,N_r]$, and $m\in[1,N_t]$ [7]. Equally important, Proposition 1 benchmarks the performance of sub-optimum but practical decoders that have lower complexity than ML. Those require $N_r\geq N_t$, and rely on the null-and-cancel decoding scheme that has been developed for layered structures in [6].

The corresponding algorithm starts with the $N_r\times N_t$ para-unitary matrix $\mathbf{Q}_g(l)$ in the QR factorization of $\mathbf{H}_g(l)=\mathbf{Q}_g(l)\mathbf{U}_g(l)$, and uses $\mathbf{Q}_g(l)$ in (5) to form the matrix $\bar{\mathbf{R}}_g(l):=\mathbf{Q}_g^{\mathcal{H}}(l)\mathbf{Y}_g(l)=\mathbf{U}_g(l)\mathbf{C}_g(l)+\mathbf{Q}_g^{\mathcal{H}}(l)\mathbf{W}_g(l)$, where $\mathbf{U}_g(l)$ is an $N_t\times N_t$ upper triangular matrix [9]. Suppose we have decoded the first $(p-1)$ layers that correspond to the first $(p-1)$ diagonals in (1). To decode the block $\mathbf{s}_g^{(p)}$, we consider the $(m,p+m-1)$ entry of $\bar{\mathbf{R}}_g(l)$ that can be written as $\bar{r}_{g,m}^{(p)}(l)=U_{g,m}(l)\boldsymbol{\theta}_{lN_t+m}^T\mathbf{s}_g^{(p)}+\mathcal{L}(\mathbf{s}_g^{(1)},\ldots,\mathbf{s}_g^{(p-1)})+v_{g,m}^{(p)}(l)$, where $\mathcal{L}(\mathbf{s}_g^{(1)},\ldots,\mathbf{s}_g^{(p-1)})$ contains symbols from previously decoded layers, and $v_{g,m}^{(p)}(l)$ denotes the $(m,m+p-1)$th entry of $\mathbf{Q}_g^{\mathcal{H}}(l)\mathbf{W}_g(l)$. If all previous layers have been decoded correctly, we can cancel the term $\mathcal{L}(\mathbf{s}_g^{(1)},\ldots,\mathbf{s}_g^{(p-1)})$ to obtain

$$\begin{aligned} r_{g,m}^{(p)}(l) :&= \bar{r}_m^{(p)}(l)-\mathcal{L}(\mathbf{s}_g^{(1)},\ldots,\mathbf{s}_g^{(p-1)}) \\ &= U_{g,m}(l)\boldsymbol{\theta}_{lN_t+m}^T\mathbf{s}_g^{(p)}+v_{g,m}^{(p)}(l). \end{aligned} \tag{6}$$

What boosts performance of the nulling-cancelling iteration in our case is the de-precoding step that is needed after the interference nulling to decode $\mathbf{s}_g^{(p)}$ from the LCP blocks $\boldsymbol{\theta}_{lN_t+m}^T\mathbf{s}_g^{(p)}$ in (6). Collecting eq. (6) for $l\in[0,L]$ and $m\in[1,N_t]$, we perform de-precoding per layer p of each group g, based on the block: $\mathbf{r}_g^{(p)}=\mathbf{D}_g^{(p)}\mathbf{\Theta}\mathbf{s}_g^{(p)}+\mathbf{v}_g^{(p)}$, where $\mathbf{D}_g^{(p)}:=\text{diag}[U_{g,1}(0)\cdots U_{g,N_t}(0)\cdots U_{g,1}(L)\cdots U_{g,N_t}(L)]$, and $\mathbf{v}_g^{(p)}\triangleq[v_{g,1}^{(p)}(0)\cdots v_{g,N_t}^{(p)}(0)\cdots v_{g,1}^{(p)}(L)\cdots v_{g,N_t}^{(p)}(L)]^T$. This step is implemented using the Sphere-Decoding (SD) algorithm that is known to exhibit near-ML performance at complexity that is polynomial in the length $N_t(L+1)$ of $\mathbf{s}_g^{(p)}$ [4]. Even lower complexity de-precoding is possible by inverting $\mathbf{\Theta}\mathbf{s}_g^{(p)}$ in the zero-forcing or minimum mean-square sense (see [7, 10] for details).

To assess the diversity order with layer decoding (that includes de-precoding), we assume that layers 1 through $p-1$ have been decoded correctly, and consider the event $\{\mathbf{s}_g^{(p)}\rightarrow\tilde{\mathbf{s}}_g^{(p)}\}$ that $\mathbf{s}_g^{(p)}$ is decoded erroneously as $\tilde{\mathbf{s}}_g^{(p)}$ during the pth layer decoding. Relying on standard Chernoff bounding techniques, we can express the average pairwise error probability as

$$\begin{aligned} &E\{P(\mathbf{s}_g^{(p)}\rightarrow\tilde{\mathbf{s}}_g^{(p)}|\{\mathbf{H}_g(l)\}_{l=0}^{L})\} \\ &\leq\prod_{i\in\mathcal{I}_g}\left(|\boldsymbol{\theta}_i^T(\mathbf{s}_g^{(p)}-\tilde{\mathbf{s}}_g^{(p)})|^2\right)^{-\mathcal{F}(i)}\left(\frac{\bar{\gamma}}{4}\right)^{-\sum_{i\in\mathcal{I}_g}\mathcal{F}(i)}, \end{aligned} \tag{7}$$

where the set of indices $\mathcal{I}_g$ is defined as $\mathcal{I}_g:=\{i:|\boldsymbol{\theta}_i^T(\mathbf{s}_g^{(p)}-\tilde{\mathbf{s}}_g^{(p)})|\neq 0\}$, $\bar{\gamma}$ is the average SNR per symbol, and $\mathcal{F}(i):=N_r-f(i)+1$ with $f(i)\equiv i\pmod{N_t}$. From (7), it can be readily seen that the *diversity order per layer* is:

$G_d^{(p)} = \sum_{i\in\mathcal{I}_g} \mathcal{F}(i)$. Next, we present our result on $G_d^{(p)}$ without accounting for error propagation when the receiver relies on layered decoding with de-precoding.

Proposition 2 *If the channel taps are i.i.d., and* $\mathbf{\Theta}$ *is selected so that* $\prod_{i=1}^{N_t(L+1)} \boldsymbol{\theta}_i^T \mathbf{e}_g^{(p)} \neq 0$, *for any* $\mathbf{e}_g^{(p)} \neq \mathbf{0}$ *with* $p \in [1, N_l]$, *and* $N_r \geq N_t$, *the layer decoding/de-precoding achieve layer diversity gain* $G_d^{(p)} = [N_r N_t - (N_t-1)N_t/2](L+1)$ *per group.*

Proof: If $\mathbf{\Theta}$ is selected so that $\prod_{i=1}^{N_t(L+1)} \boldsymbol{\theta}_i^T \mathbf{e}_g^{(p)} \neq 0$, $\forall\ \mathbf{e}_g^{(p)} \neq \mathbf{0}$, then $\mathcal{I}_g = \{1, \ldots, N_t(L+1)\}$. It thus follows from (7) that $G_d^{(p)} = \sum_{i\in\mathcal{I}_g} \mathcal{F}(i) = \sum_{i=1}^{N_t(L+1)} [N_r - f(i) + 1]$. As $f(i) \equiv i \pmod{N_t}$, it can be easily seen that $\sum_{i=1}^{N_t(L+1)} [N_r - f(i) + 1] = N_r N_t(L+1) - (L+1)(N_t-1)N_t/2$. □

It is worth noting that $G_d^{(p)}$ does not depend on p. This is in agreement with the original DBLAST scheme applied to flat-fading channels, where the order of decoding the layers does not affect decoding performance [6].

In order to maximize the diversity order, Propositions 1 and 2 suggest designing the LCP matrix $\mathbf{\Theta}$ such that $\prod_{i=1}^{N_t(L+1)} \boldsymbol{\theta}_i^T \mathbf{e}_g^{(p)} \neq 0$, $\forall\ \mathbf{e}_g^{(p)} \neq \mathbf{0}$, and $\forall\ p \in [1, N_l]$. Fortunately, $\mathbf{\Theta}$'s satisfying this condition for any value of $N_t(L+1)$ are possible, and can be found in [10, eq. (7)].

Fig. 2 depicts the performance comparison between DBLAST-OFDM-LCP and VBLAST-OFDM. Using $N_c = 15$ and $L = 2$, we test two cases for $N_t = N_r = 5$, and $N_t = N_r = 3$ with 16-QAM. We use Reed-Solomon (15,9) codes for VBLAST-OFDM, and the precoder $\mathbf{\Theta}$ of [10, eq. (7)] for DBLAST-OFDM-LCP. Since the transmit-diversity order is high for $N_t = N_r = 5$, we use the sub-optimum precoder $\tilde{\mathbf{\Theta}}$ to reduce the complexity at the expense of multipath-diversity loss (see discussion before (1)). To ensure identical transmission rates for VBLAST-OFDM and DBLAST-OFDM-LCP, we choose $N = 5$ when $N_t = N_r = 3$, and $N = 10$, when $N_t = N_r = 5$. The corresponding rates are $R = 6.35$ bps/Hz, and $R = 10.58$ bps/Hz, respectively. Fig. 2 corroborates that DBLAST-OFDM-LCP outperforms VBLAST-OFDM considerably (about 5 dB at BER $= 10^{-4}$).

In the full version of this work, we will study the performance with error propagation in the decoding process. We will also assess the coding gains along with the pertinent complexity-performance-rate tradeoffs. Finally, we will explore alternative high-rate schemes, not only for multi-carrier, but also for single-carrier multi-antenna systems as well as for ST transmissions that allow operation even with $N_r < N_t$.

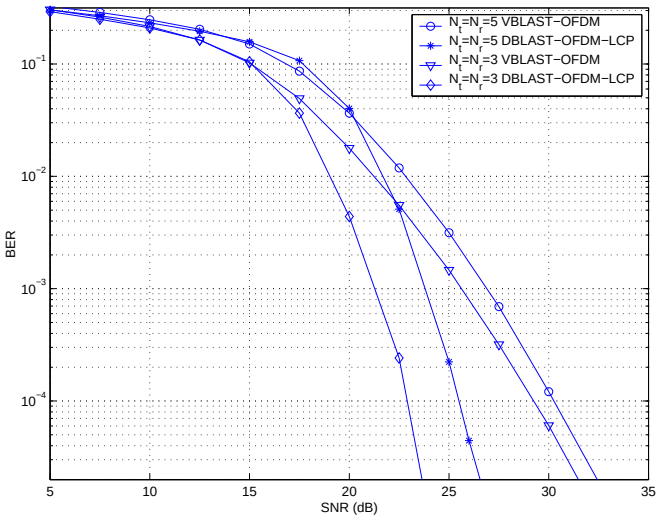

Figure 2: DBLAST-OFDM-LCP vs. VBLAST-OFDM

References

[1] D. Agrawal, V. Tarokh, A. Naguib, and N. Seshadri, "Space-time coded OFDM for high data-rate communication over wideband channels, " in *Proc. Vehicular Technology Conf.*,, Ottawa, ON, Canada, May 18-21, 1998, pp. 2232-2236.

[2] S. L. Ariyavisitakul, "Turbo space-time processing to improve wireless channel capacity," *IEEE Trans. on Communications*, vol. 48, no. 8, pp. 1347-1359, Aug. 2000.

[3] R. S. Blum, Y. Li, J. H. Winters, and Q. Yan, "Improved space-time coding for MIMO-OFDM wireless communications," *IEEE Trans. on Communications*, vol. 49, no. 11, pp. 1873-1878, Nov. 2001.

[4] J. Boutros and E. Viterbo, "Signal space diversity: A power and bandwidth efficient diversity technique for the Rayleigh fading channel," *IEEE Trans. on Information Theory*, vol. 44, no.4, pp. 1453-1467, July 1998.

[5] G. J. Foschini and M. J. Gans, "Layered space-time architecture for wireless communication in a fading environment when using multiple antennas," *Bell Labs. Syst. Tech. J.*, vol. 1, pp. 41-59, Autumn 1996.

[6] G. J. Foschini, G. D. Golden, R. A. Valenzuela, and P. W. Wolniansky, "Simplified processing for high spectral efficiency wireless communication employing multi-element arrays," *IEEE J. on Selected Areas in Comm.*, vol. 17, no. 11, pp. 1841-1852, Nov. 1999.

[7] Z. Liu, Y. Xin, and G. B. Giannakis, "Space-Time-Frequency Coded OFDM over Frequency-Selective Fading Channels," *IEEE Transactions on Signal Processing*, 2002; see also *Proc. of Intl. Conf. on ASSP*, Orlando, FL, May 13-17, 2002. downloadable from `http://spincom.ece.umn.edu/yxin/STF.pdf`.

[8] R. J. Piechocki, P. N. Flectcher, A. R. Nix, C. N. Canagarajah, and J. P. McGeehan, "Performance evaluation of BLAST-OFDM enhanced Hiperlan/2 using simulated and measured channel data," *Electronics Letters*, vol. 37, No. 18, pp. 1137-1139, Aug. 2001.

[9] D. Shiu and J. M. Kahn, "Scalable layered space-time codes for wireless communications: performance analysis and design criteria," in *Proc. of Wireless Communications and Networking Conf.,* New Orleans, LA, September 21-24, 1999, pp. 159-163. Journal submission downloadable from `http://www.cs.berkeley.edu/~jmk//res.areas/`

[10] Y. Xin, Z. Wang, and G. B. Giannakis, "Space-time constellation-rotating codes maximizing diversity and coding gains," in *Proc. of GLOBECOM Conf.*, San Antonio, TX, Nov. 25-29, 2001, pp. 455-459.